Nuclear Inst. and Methods in Physics Research, A 1047 (2023) 167779

Contents lists available at ScienceDirect

Nuclear Inst. and Methods in Physics Research, A

journal homepage: www.elsevier.com/locate/nima

Performance evaluation of 3D median modified Wiener filter in brain T1-weighted magnetic resonance imaging

Dohwa Lee [a], Chang-Soo Yun [b], Seong-Hyeon Kang [a,c], Minji Park [a,c], Youngjin Lee [a,*]

[a] Department of Radiological Science, College of Health Science, Gachon University, 191, Hambakmoero, Yeonsu-gu, Incheon, Republic of Korea
[b] Department of Radiation Convergence Engineering, College of Software and Digital Healthcare Convergence, Yonsei University, 1, Yeonsedae-gil, Heungeop-myeon, Wonju, Gangwon-do, Republic of Korea
[c] Department of Health Science, General Graduate School of Gachon University, 191, Hambakmoe-ro, Yeonsu-gu, Incheon, Republic of Korea

ARTICLE INFO

Keywords:
T1-weighted magnetic resonance brain image
Noise reduction filter
3D median modified wiener filter (MMWF)
BrainWeb simulated brain MRI database
Alzheimer's disease neuroimaging initiative (ADNI) database
Quantitative evaluation of image quality

ABSTRACT

The purpose of this study aimed to evaluate the noise reduction efficiency of a 3D median modified Wiener filter (MMWF) in brain T1-weighted magnetic resonance (MR) images. A simulation using BrainWeb phantom data and real experimental research based on data of the Alzheimer's Disease Neuroimaging Initiative (ADNI) were performed, and the 2D MMWF was modeled to prove the usefulness of the proposed 3D MMWF. Brain MR images were obtained according to the kernel size and noise level of 2D and 3D MMWF, and the coefficient of variation (COV) and edge preservation index (EPI) were used for the quantitative evaluation of the obtained images. According to the changes in COV with respect to the changes in filter size, simulated T1-weighted images with 3D MMWF had a 2.76 times higher denoising performance than 2D MMWF. Furthermore, the EPI of simulated T1 weighted images with 3D MMWF had a 1.17 times better performance than that of simulated T1-weighted images with 2D MMWF, particularly in noisy images. To confirm the performance of 3D MMWF with clinical T1-weighted images, we obtained a T1-weighted image from ADNI and applied 2D and 3D MMWF with respect to kernel size. According to COV changes with respect to kernel size in both filters, clinical T1-weighted images showed a 1.14 times improvement with 3D MMWF and had a similar tendency as simulated images. We compared 2D and 3D MMWF in terms of tissue preservation and denoising performance in T1-weighted images. Our results indicate that the proposed 3D MMWF has better denoising performance than 2D MMWF for Rician noise and preserved the edges of brain tissues.

1. Introduction

In the medical fields, magnetic resonance imaging (MRI) has high spatial resolution and can provide contrast enhancement for the diagnosis of lesions in soft tissue, particularly the brain. Appropriate image acquisition parameter should be used not only investigation of the exact location of the lesion but also determination of the characteristic of region of interest (ROI). T1-weighted image is one of the representative sequences in MRI acquisition that use short time repetition and time of echo. T1-weighted images provide the accurate brain segmentation for functional MRI (fMRI) or diffusion MRI (dMRI) and the course of the disease (e.g., Parkinson's disease, Alzheimer's disease, and cerebral infraction) [1–4].

Rician noise is generated during MRI acquisition, and it disturbs the location of brain lesions and reduces the accuracy of disease diagnosis. Thermal noise generated by the human body and magnetic resonance (MR) equipment affects the real and imaginary parts of k-space data as white noise with Gaussian distribution. MRI reconstructs the k-space data affected by thermal noise by using inverse Fourier transform. These effects are expressed as Rayleigh and Gaussian distributions in MRI, and the combined form is called Rician noise [5–7]. Research of filtering-based, transform domain, and statistical approach image filters have been conducted to remove Rician noise in MRI [8,9]. Representatively, linear filters (Gaussian, mean filter) and non-linear filters (non-local mean, weighted median filter, and adaptive Wiener filter) are widely used to remove the Rician noise in MRI. Median filter applies the median value of the ROI preserves the high frequency signal of the medical image but increasing the blurring effect [10]. In addition, a Wiener filter minimizes the squared error between the reference image and the reconstructed image [11]. According to Ali et al. [12], image noise was effectively reduced when the above-mentioned filters were applied to MRI performed using various imaging techniques. Although image filters effectively reduce the noise of images, such filters increase the blurring effect of MRI, and cause loss of information and sharpness between tissues [13].

To solve this problem, Cannistraci et al. [14] proposed the 2D median modified Wiener filter (MMWF), which is a combination of

* Corresponding author.
E-mail address: yj20@gachon.ac.kr (Y. Lee).

https://doi.org/10.1016/j.nima.2022.167779
Received 8 August 2022; Received in revised form 17 October 2022; Accepted 7 November 2022
Available online 15 November 2022

Table 1
Acquisition of T1-weighted image parameters from the BrainWeb and ADNI database.

T1-weighted image	Noise level	TR	TE	Flip angle	Slice thickness	Pulse sequence
BrainWeb database	0% 1% 3% 5% 7% 9%	6.8 ms	3.2 ms	9 degrees	1.2 mm	Simulated fast low-angle shot
ADNI database	–					Gradient echo

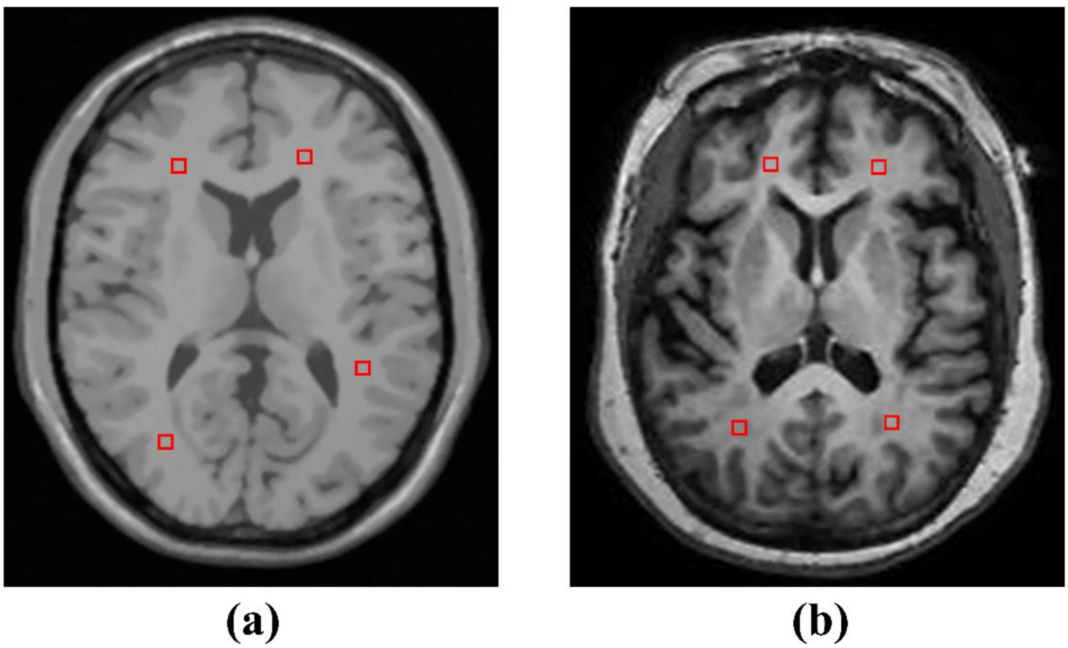

Fig. 1. Sample T1-weighted images obtained from (a) BrainWeb and the (b) ADNI clinical database. Region of interest (ROI) using box type were illustrated for calculating the coefficient of variation (COV).

median and Wiener filters. 2D MMWF not only maintains the edges of structural images but also reduces the image noise. Until recently, research has been conducted on noise removal by applying 2D MMWF to diagnostic medical images [15–19]. According to Lee et al. [16], application of 2D MMWF to an X-ray image improved the contrast-to-noise ratio (CNR) by 1.08 times, the coefficient of variation (COV) by 1.10 times, and blind/referenceless image spatial quality evaluator by 1.03 times compared with those of the obtained image. Furthermore, Kim et al. [15], applied 2D MMWF to a single photon emission computed tomography (SPECT) image and obtained enhancements of 35.9% and 17.1% in signal-to-noise ratio (SNR) and CNR, respectively. Choi et al. [19] verified that 2D MMWF has better performance in maintaining the similarity and noise evaluation index than median and Wiener filters in T2-weighted images. Therefore, the proper use of 2D MMWF in medical images, including MRI scans, could reduce the noise in images and preserve the edges of tissues.

However, MRI represents complicated 3D anatomical structures; therefore, the preservation of the spatial information of images is not efficient when a 2D noise removal algorithm is applied [20]. Therefore, 3D noise reduction image filters should be designed for the preservation of edge structural regions and minimization of the image distortion of signal intensity. Cannistraci et al. [21] proposed the 3D MMWF to reduce the noise of nuclear MR signals from raw data. Therefore, it is necessary to evaluate the performance of reducing Rician noise using 3D MMWF, which has the advantages of 3D image filter.

In this study, we compared the Rician denoising performance between 2D and 3D MMWF in T1-weighted images using data from BrainWeb simulations and the Alzheimer's Disease Neuroimaging Initiative (ADNI). To evaluate the denoising performance, various image quality evaluation factors were used for the comparative evaluation between 2D and 3D MMWF.

2. Materials and methods

2.1. Simulation of brain T1-weighted image using various acquisition parameter from BrainWeb database

BrainWeb, which is a simulation program, can adjust the various MRI acquisition parameter [22]. Simulated T1-weighted images of the brain were acquired with respect to Rician noise level for evaluating the denoising performance of 2D and 3D MMWF. In addition, a clinical T1-weighted image was obtained from the ADNI database [23] to observe whether denoising performance has a similar tendency when the 2D and 3D MMWF were applied to clinical data. Table 1 shows the image acquisition parameters.

2.2. Proposed 3D MMWF modeling

To evaluate the denoising performance of 3D MMWF, 2D MMWF proposed by Cannistraci et al. [14] was applied as follows before modeling the image filter:

$$b_{mmwf}(x, y) = \overline{\mu} + \frac{\sigma^2 - \gamma^2}{\sigma^2} \cdot \left(A(x, y) - \overline{\mu}\right), \tag{1}$$

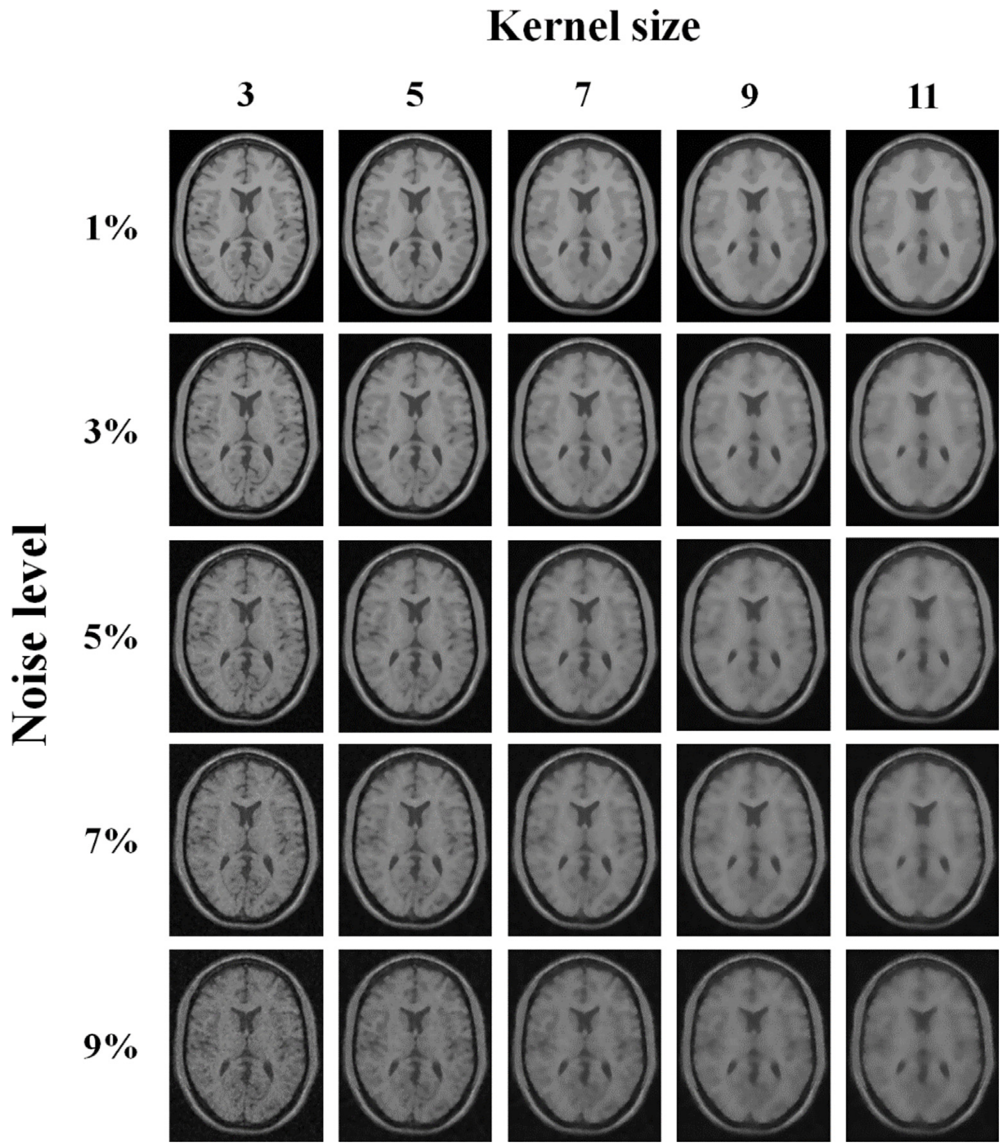

Fig. 2. Results of simulated T1-weighted images obtained from BrainWeb with respect to kernel size for 2D MMWF using various noise levels.

where $\overline{\mu}$ and σ denote the median and standard deviation value of the kernel, respectively; γ^2 is the standard deviation of noise; and $A(x, y)$ is the signal intensity of the (x, y) area. On the basis of the 2D MMWF equation, 3D MMWF, which additionally reflects the pixels of the 3D area $A(x, y, z)$, was modeled as follows:

$$b_{mmwf}(x, y, z) = \overline{\mu} + \frac{\sigma^2 - \gamma^2}{\sigma^2} \cdot \left(A(x, y, z) - \overline{\mu}\right), \tag{2}$$

Kernel sizes were applied as 3, 5, 7, 9, and 11 in the 2D and 3D MMWF.

2.3. Quantitative evaluation of image quality

COV was measured for quantitative noise evaluation factors to compare the performance between 2D and 3D MMWF in simulations and clinical T1-weighted images. In addition, the edge preservation index (EPI) was measured to evaluate the restoration of tissue edges in a simulated T1-weighted image. To evaluate the COV, the ROI in white matter was annotated using a simulated T1-weighted image (Fig. 1). Furthermore, a sliced image used to calculate the EPI. COV is a quantitative index that is used for comparing image noise in ROI (Eq. (3)), and a lower COV value is correlated with better image quality.

$$COV = \frac{\sigma_A}{S_A}, \tag{3}$$

where S_A and σ_A denote the signal intensity of ROI and the standard deviation of image noise, respectively.

EPI is an index for observing similarity (Eq. (4)) and was used to compare the edges of tissues between the reference images (e.g., Rician noise is not included), and 3D MMWF was applied to simulated T1-weighted images. EPI was measured as a value between 0 and 1: an EPI close to 1 means that the edges of the reference image and the noisy image with the denoising filter are similar.

$$EPI = \frac{\Gamma(\Delta q_1 - \overline{\Delta q_1}, \Delta q_2 - \overline{\Delta q_2})}{\Gamma(\Delta q_1 - \overline{\Delta q_1}, \Delta q_1 - \overline{\Delta q_1}) \cdot \Gamma(\Delta q_2 - \overline{\Delta q_2}, \Delta q_2 - \overline{\Delta q_2})}, \tag{4}$$

where $\overline{\Delta q}$ was calculated after application of the Laplacian filter by using 0.3 in ROI, and q_1 and q_2 denote the reference image and the image with the filter, respectively.

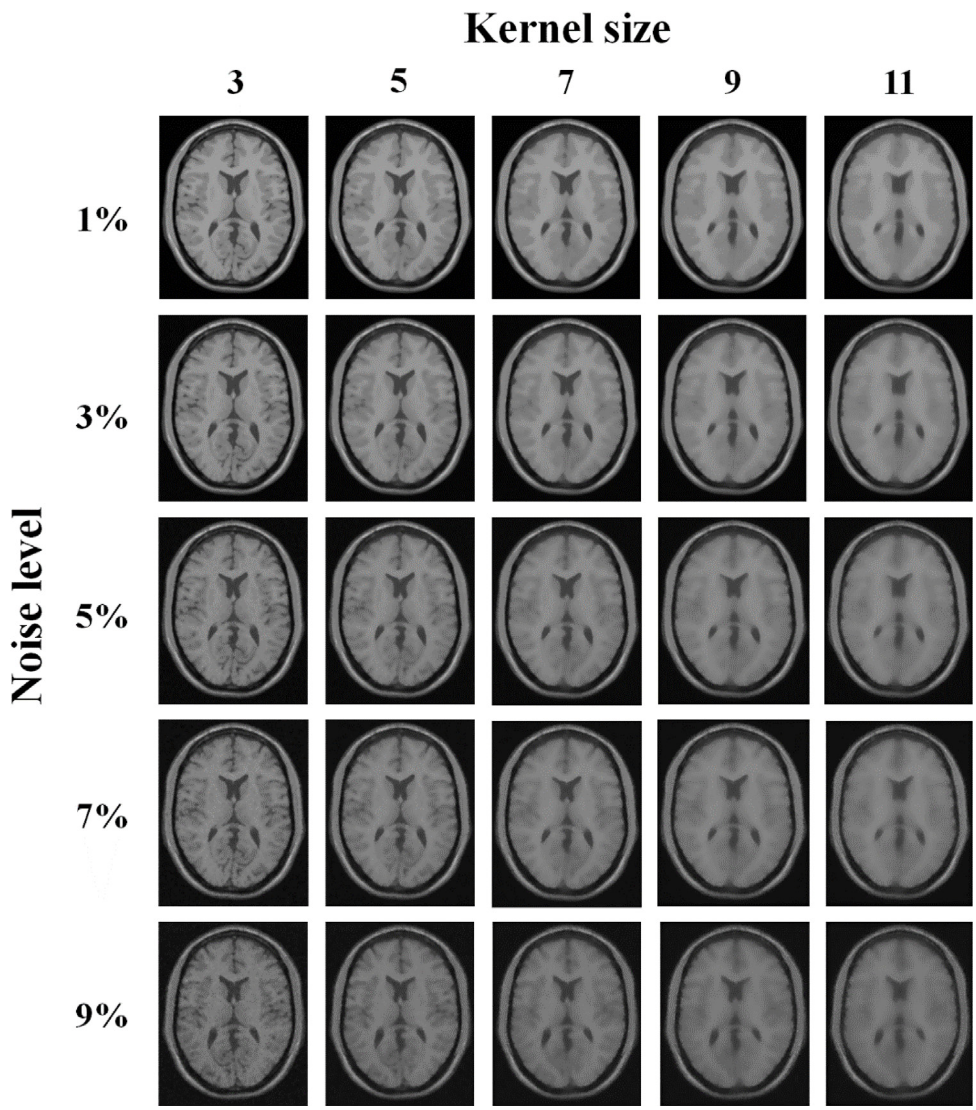

Fig. 3. Results of simulated T1-weighted images obtained from BrainWeb with respect to kernel size for 3D MMWF using various noise levels.

3. Results and discussions

MRI is a useful technique for identifying the course of a disease and determining the exact location of a lesion in brain diseases. T1-weighted images is used to determine the exact structural location of a lesion in the brain. When acquiring fMRI and dMRI, it is necessary to acquire T1-weighted images in order to identify the exact structural location of brain lesions. However, Rician noise in T1-weighted image interferes with the accurate anatomical segmentation of brain regions, which could cause serious problems in brain surgery or radiation therapy. Therefore, removing Rician noise in MRI play important roles in finding the precise location of a lesion.

2D MMWF has better performance in reducing Rician noise in T2-weighted images in COV [19]. However, 2D MMWF uses neighborhood pixels for denoising in MRI but does not use the pixels of other slices as references. As a result, 2D MMWF can be effective in preserving large-scale structures similar to other 2D denoising image filters but may incorrectly identify the small structures of brain tissue as noise when an image filter is applied [24]. To solve this problem, Coupe et al. [6] proposed a 3D NLM image filter that uses the similar 3D neighbor of voxels as references by using two voxels to reduce image noise. In addition, diverse methods have been developed to apply a denoising filter to 3D images to maintain noise efficiency and edges of tissues in medical images [24–27]. According to Cannistraci et al. [21], 3D MMWF was proposed to remove noise in multidimensional nuclear MR spectra in raw data areas. The application of 3D MMWF to nuclear MR spectra has led to improvements in the detection of spectrum signal compared with the 2D MMWF applied. Despite the advantages of 3D MMWF, studies have not been conducted on the removal of image noise by using 3D MWMF on medical images.

We evaluated the denoising performance of 3D MMWF by using different kernel sizes in simulated and clinical T1-weighted images. To observe the denoising efficiency of 3D MMWF, brain T1-weighted images with 1%, 3%, 5%, 7%, and 9% Rician noise levels were simulated using BrainWeb. Figs. 2 and 3 respectively show the 2D and 3D MMWF that were applied to the simulated images with respect to kernel size. Image blur increased as the kernel size increased regardless of the amount of Rician noise. Additionally, to evaluate the denoising performance of both image filters, the variation of COV with respect to the filter size was calculated. Fig. 4 shows the results of this calculation. COV decreased as kernel size increased regardless of the amount of Rician noise. After application of 2D MMWF, COV with respect to kernel sizes of 3, 5, 7, 9, and 11 in simulated T1-weighted images with a 1% Rician noise level increased by 1.49, 1.69, 1.72, 1.51, and 1.40 times, respectively, compared with those after application of 3D MMWF. However, the COV of simulated T1-weighted images applied with 2D MMWF and with a 9% Rician noise level are 1.59, 2.17, 2,43, 2,76, and 2.26 times higher than that with 3D MMWF, respectively.

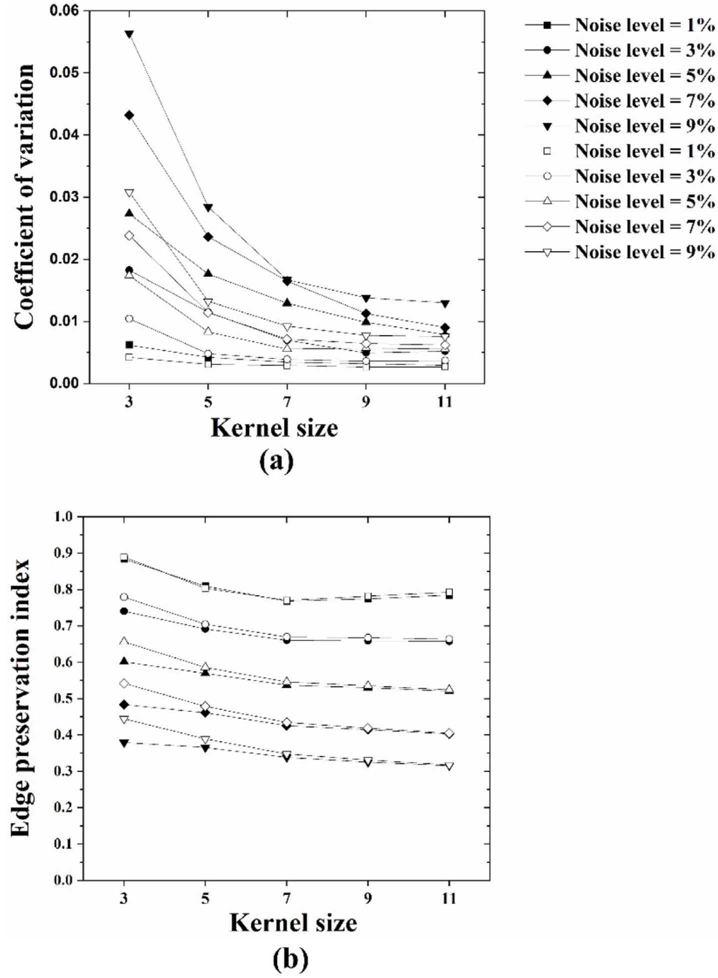

Fig. 4. Graph results for the evaluated (a) coefficient of variation (COV) and (b) edge preservation index (EPI) with respect to kernel size for 2D and 3D MMWF (black and white diagrams, respectively) in simulated T1-weighted images using BrainWeb.

According to the results of COV, it can be confirmed that the Rician noise denoising performance of 3D MMWF is superior to that of 2D MMWF in simulated T1-weighted images with a high amount of Rician noise. To observe the changes of edges between brain tissues due to the blurring effect from a denoising image filters, EPI was calculated using simulated T1-weighted images with 2D and 3D MMWF, and Fig. 4(b) shows the tendency of EPI changes. The low amount of Rician noise in the simulated T1-weighted image shows that EPI has minor changes in both image filters regardless of kernel size. However, by application of a small kernel size to a simulated T1-weighted image with a high Rician noise level, a higher EPI can be measured in 3D MMWF than 2D MMWF. According to the EPI results, the application of 3D MMWF to T1-weighted images changes the EPI values with respect to kernel sizes of 3, 5, 7, 9, and 11 with a 1% Rician noise to 1.01, 1.00, 1.01, 1.02, and 1.02 times higher than the EPI values with the application of 2D MMWF. However, simulated T1-weighted images with a 9% Rician noise level and 3D MMWF have EPI values that are 1.17, 1.03, 1.01, 1.00, and 1.00 times higher than those with 2D MMWF. According to this tendency of EPI, the use of a small kernel size in 3D MMWF can better preserve the edge of tissues in low Rician noise in simulated T1-weighted images than 2D MMWF.

To observe the tendency of 2D and 3D MMWF regardless of the amount of Rician noise in T1-weighted images, five difference kernels were applied in each image filter to calculate the average COV and EPI (Fig. 5). The average of EPI in 2D and 3D MMWF had similar tendencies regardless of kernel size (Fig. 5b), and the average of COV in 3D MMWF was lower than that in 2D MMWF (Fig. 5a). It is necessary to confirm whether the noise evaluation factor calculated after application of 2D and 3D MMWF to clinical T1-weighted images has a similar tendency to the result of the noise evaluation factor in simulated T1-weighted images. Therefore, the clinical T1-weighted image obtained from the ADNI database is used for the evaluation of COV with respect to changes in filter kernel size (Fig. 6), and the noted area is used for calculating COV. It was impossible to obtain a noise free image (e.g., reference image) in a clinical image because EPI was not calculated in a clinical T1-weighted image. Therefore, COV was calculated in a clinical T1-weighted image in accordance with kernel size (Fig. 7). Given that the amount of Rician noise was low in a simulated T1-weighted image in which random Rician noise was applied, the COV of the two denoising filters tended to be similar as the kernel size increased. Regarding the changes in COV with kernel size, 3D MMWF had COV that are 1.14, 1.10, 1.12, 1.08, and 0.98 times higher than those of 2D MMWF. When denoising Rician noise using a small kernel size of 3, a clinical T1-weighted image applied with the 3D MMWF showed more improvements in noise reduction than that applied with the 2D MMWF. Compared with the result of a simulated T1-weighted image, 3D MMWF was more efficient in removing Rician noise and in preserving the edges of tissues in brain image. Furthermore, a similar tendency was observed in simulated T1-weighted images with both image filters. Despite the higher Rician noise in T1-weighted images, 3D MMWF showed similar or better edge preservation of tissues and denoising performance than 2D MMWF in simulated and clinical T1-weighted images.

Denoising performance was evaluated using the proposed 3D MMWF in T1-weighted images obtained from BrainWeb and the ADNI

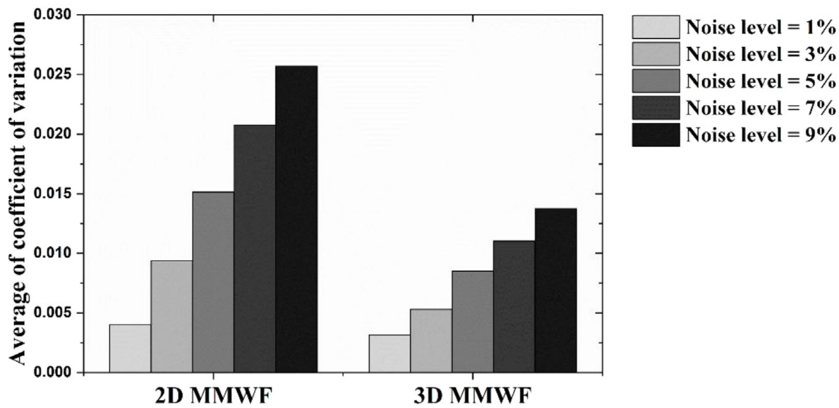

(a)

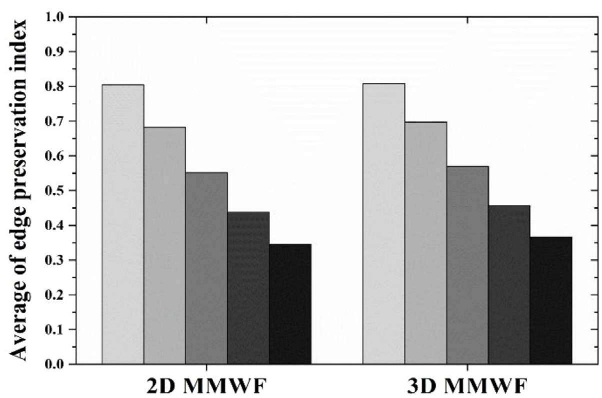

(b)

Fig. 5. Average of (a) COV and (b) EPI after application of the five different kernel sizes of 2D and 3D MMWF with respect to noise level.

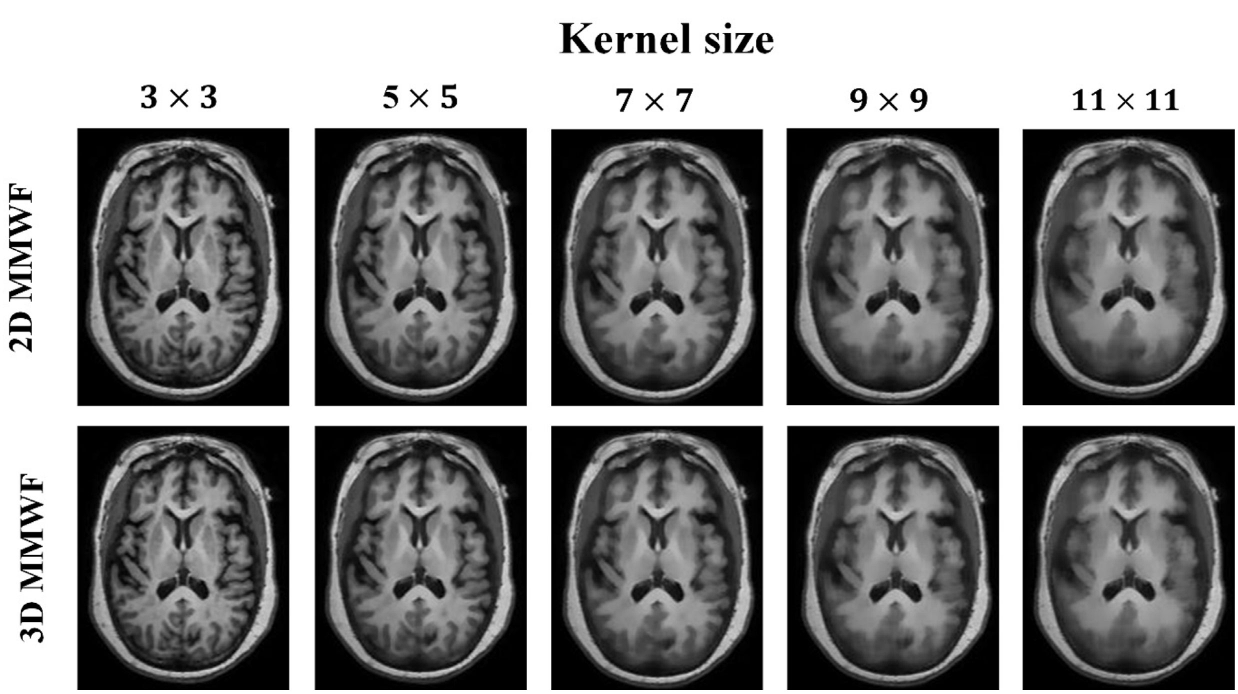

Fig. 6. Results of T1-weighted images obtained from the ADNI database with respect to kernel size for 2D and 3D MMWF.

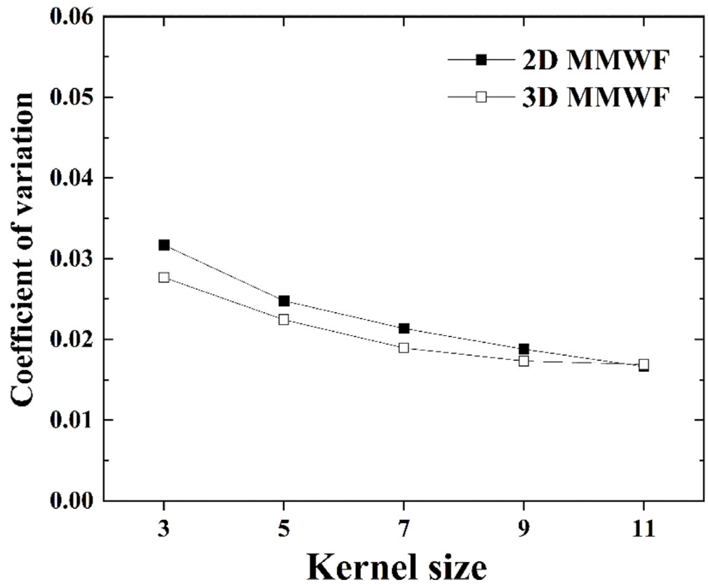

Fig. 7. Results of coefficient of variation (COV) with respect to kernel size for 2D and 3D MMWF in clinical T1-weighted image obtained from the ADNI database.

database. For the average of COV and EPI with a specific noise level regardless of kernel size, 3D MMWF had better denoising performance that can be inferred with COV. Preserving the edges of brain tissues inferred with EPI was more efficient preventing the increase in the blurring effect of the image. These results show that the 3D MMWF had better performance in denoising simulated and clinical T1-weighted images and was more efficient in reducing the blurring effect of the images than the 2D MMWF.

To reduce noise in medical images, various studies on denoising using conventional image filters have been performed to improve image quality and increase diagnosis accuracy. In recent years, the development of deep learning algorithms for image denoising has increased. Other medical imaging techniques such as computed tomography and SPECT are indispensable when using image denoising filters to trade off the radiation dose. MRI does not emit ionizing radiation but has a longer acquisition time than other medical imaging techniques. A long acquisition time causes motion artifacts and increases the probability of generating image noise, which interferes with determining the location of a lesion for diagnosis [28–30]. Motion artifacts in MRI interrupts brain segmentation, which can cause misdiagnoses in surgery or radiation therapy. Currently, the application of a software-based image filter to medical images is important for increasing the accuracy of deep learning algorithms in making diagnoses, particularly with regard to diseases involving the brain. To predict a disease using deep learning methods in the medical image field, various denoising methods are used to improve the model accuracy. According to Lee et al. [31], ^{18}F-positron emission tomography (^{18}F-PET) image is used for deep learning models to predict Alzheimer's disease. Notably, ^{18}F-PET images that use 2D MMWF for preprocessing have better accuracy for the diagnosis of Alzheimer's disease. The prediction model of deep learning methods for the denoising of medical images improves the accuracy of disease diagnosis, particularly when using MRI to diagnose Alzheimer's disease [32–34]. Therefore, 3D MMWF is not only effective in removing Rician noise but also in preserving the edges of brain tissues in MRI, has the advantage of improving the accuracy of diagnosis by preserving small brain structures, and can increase the accuracy of deep learning models that are used in identifying minute changes in the brain.

4. Conclusion

In this study, we evaluated the denoising performance between 2D and 3D MMWF using T1-weighted images. 3D MMWF has better performance than 2D MMWF regardless of the amount of Rician noise in the images. When applied to T1-weighted images with 9% Rician noise using 3D MMWF with a small kernel size, COV and EPI have 1.49 and 1.17 times improvement than 2D MMWF. In addition, when appropriate kernel size of 3D MMWF is applied to T1-weighted images with 1% Rician noise, EPI shows a similar tendency in both image filter, but COV improved up to 1.72 times than 2D MMWF.

According to our results, 3D MMWF provides better image restoration than 2D MMWF at reducing Rician noise while preserving the edges of the T1-weighted images. Therefore, the denoising of MRI using 3D MMWF is expected to improve the accuracy of deep learning models that are designed for diagnosing various brain diseases and lesions. Furthermore, 3D MMWF can be used with diverse MRI techniques to improve the diagnostic accuracy of fMRI or dMRI. In future studies, we will observe if diagnostic accuracy can be improved by application of 3D MMWF to MRI of various brain diseases and by using a deep learning model.

Declaration of competing interest

The authors declare that they have no known competing financial interests or personal relationships that could have appeared to influence the work reported in this paper.

Data availability

No data was used for the research described in the article.

References

[1] K. Morgen, G. Sammer, L. Weber, B. Aslan, C. Müller, G.F. Bachmann, D. Sandmann, M. Oechsner, D. Vaitl, M. Kaps, I. Reuter, Structural brain abnormalities in patients with Parkinson disease: A comparative voxel-based analysis using T1-weighted MR imaging and magnetization transfer imaging, AJNR Am. J. Neuroradiol. 32 (2011) 2080–2086.

[2] C. Platero, M.E. López, M.D. Carmen Tobar, M. Yus, F. Maestu, Discriminating Alzheimer's disease progression using a new hippocampal marker from T1-weighted MRI: The local surface roughness, Hum. Brain Mapp. 40 (2019) 1666–1676.

[3] J.B. Allendorfer, B.M. Kissela, S.K. Holland, J.P. Szaflarski, Different patterns of language activation in post-stroke aphasia are detected by overt and covert versions of the verb generation fMRI task, Med. Sci. Monit. Int. Med. Exp. Clin. Res. 18 (2012) CR135.

[4] M. Malinsky, R. Peter, E. Hodneland, A.J. Lundervold, A. Lundervold, J. Jan, Registration of FA and T1-weighted MRI data of healthy human brain based on template matching and normalized cross-correlation, J. Digit. Imaging 26 (2013) 774–785.
[5] H. Gudbjartsson, S. Patz, The Rician distribution of noisy MRI data, Magn. Reson. Med. 34 (1995) 910–914.
[6] P. Coupé, J.V. Manjón, E. Gedamu, D. Arnold, M. Robles, D.L. Collins, Robust Rician noise estimation for MR images, Med. Image Anal. 14 (2010) 483–493.
[7] J. Yang, J. Fan, D. Ai, S. Zhou, S. Tang, Y. Wang, Brain MR image denoising for Rician noise using pre-smooth non-local means filter, Biomed. Eng. Online 14 (2015) 1–20.
[8] S. Kaur, J. Singla, Nikita, A. Singh, Review on medical image denoising techniques, in: 2021 International Conference on Innovative Practices in Technology and Management, ICIPTM, IEEE, 2021, pp. 61–66.
[9] J. Mohan, V. Krishnaveni, Y. Guo, A survey on the magnetic resonance image denoising methods, Biomed. Signal Process. Control 9 (2014) 56–69.
[10] S.V.M. Sagheer, S.N. George, A review on medical image denoising algorithms, Biomed. Signal Process. Control 61 (2020) 102036.
[11] T. Loupas, W.N. Mcdicken, P.L. Allan, An adaptive weighted median filter for speckle suppression in medical ultrasonic images, IEEE Trans. Circuits Syst. 36 (1989) 129–135.
[12] H.M. Ali, MRI medical image denoising by fundamental filters, High-Resolut. Neuroimaging Basic Phys. Princ. Clin. Appl. 14 (2018) 111–124.
[13] M.E. Osadebey, M. Pedersen, Arnold. D.L., K.E. Wendel-Mitoraj, Blind blur assessment of MRI images using parallel multiscale difference of Gaussian filters, Biomed. Eng. Online 17 (2018) 1–22.
[14] C.V. Cannistraci, F.M. Montevecchi, M. Alessio, Median-modified Wiener filter provides efficient denoising, preserving spot edge and morphology in 2-DE image processing, Proteomics 9 (2009) 4908–4919.
[15] E.S. Kim, Y. Lee, C.R. Park, Feasibility of MMWF noise reduction algorithm in brain SPECT images according to various reconstruction methods: A phantom study, Optik 247 (2021) 167909.
[16] S. Lee, Y. Lee, Performance evaluation of median-modified Wiener filter algorithm in high-resolution complementary metal–oxide–semiconductor radio-magnetic X-ray imaging system: An experimental study, Nucl. Instrum. Methods Phys. Res. A 1010 (2021) 165509.
[17] S. Ju, S.H. Kang, Y. Lee, Optimization of mask size for median-modified Wiener filter according to matrix size of computed tomography images, Nucl. Instrum. Methods Phys. Res. A 1010 (2021) 165508.
[18] C.R. Park, S.H. Kang, Y. Lee, Median modified wiener filter for improving the image quality of gamma camera images, Nucl. Eng. Technol. 52 (2020) 2328–2333.
[19] D. Choi, S.H. Kang, C.R. Park, Y. Lee, Study of the noise reduction algorithm with median modified wiener filter for T2-weighted magnetic resonance brain images, J. Magn. 26 (2021) 50–59.
[20] K. Dabov, A. Foi, V. Katkovnik, K. Egiazarian, Image denoising by sparse 3-D transform-domain collaborative filtering, IEEE Trans. Image Process. 16 (2007) 2080–2095.
[21] C.V. Cannistraci, A. Abbas, X. Gao, Median modified Wiener filter for nonlinear adaptive spatial denoising of protein NMR multidimensional spectra, Sci. Rep. 5 (2015) 1–8.
[22] R.K. Kwan, A.C. Evans, G.B. Pike, MRI simulation-based evaluation of image-processing and classification methods, IEEE Trans. Med. Imaging 18 (1999) 1085–1097.
[23] R.C. Petersen, P.S. Aisen, L.A. Beckett, M.C. Donohue, A.C. Gamst, D.J. Harvey, C.R. Jack, W.J. Jagust, L.M. Shaw, A.W. Toga, J.Q. Trojanowski, M.W. Weiner, Alzheimer's disease neuroimaging initiative (ADNI): clinical characterization, Neurology 74 (2010) 201–209.
[24] H. Liu, C. Yang, N. Pan, E. Song, R. Green, Denoising 3D MR images by the enhanced non-local means filter for Rician noise, Magn. Reson. Imaging 28 (2010) 1485–1496.
[25] P. Qiu, P.S. Mukherjee, Edge structure preserving 3D image denoising by local surface approximation, IEEE Trans. Pattern Anal. Mach. Intell. 34 (2012) 1457–1468.
[26] M. Hasan, M.R. El-Sakka, Improved BM3D image denoising using SSIM-optimized Wiener filter, EURASIP J. Image Video Process. (2018) 1–12.
[27] F. Romdhane, F. Benzarti, H. Amiri, 3D medical images denoising, in: International Image Processing, Applications and Systems Conference, IEEE, 2014, pp. 1–5.
[28] M. Kidoh, K. Shinoda, M. Kitajima, K. Isogawa, M. Nambu, H. Uetani, K. Morita, T. Nakaura, M. Tateishi, Y. Yamashita, Y. Yamashita, Deep learning based noise reduction for brain MR imaging: Tests on phantoms and healthy volunteers, Magn. Reson. Med. Sci. 19 (2020) 195.
[29] T. Higaki, Y. Nakamura, F. Tatsugami, T. Nakaura, K. Awai, Improvement of image quality at CT and MRI using deep learning, Jpn. J. Radiol. 37 (2019) 73–80.
[30] J.M. Shim, Y.B. Kim, C.K. Kang, Artifact reduction in compressed sensing averaging techniques for high-resolution magnetic resonance images, Appl. Sci. 11 (2021) http://dx.doi.org/10.3390/app11219802.
[31] M.H. Lee, C.S. Yun, K. Kim, Y. Lee, Effect of denoising and deblurring18 F-Fluorodeoxyglucose positron emission tomography images on a deep learning model's classification performance for Alzheimer's disease, Metabolites 12 (2022) 231, http://dx.doi.org/10.3390/metabo12030231.
[32] M. Odusami, R. Maskeliūnas, R. Damaševičius, T. Krilavičius, Analysis of features of Alzheimer's disease: Detection of early stage from functional brain changes in magnetic resonance images using a finetuned ResNet18 network, Diagnostics 11 (2021) http://dx.doi.org/10.3390/diagnostics11061071.
[33] E. Hussain, M. Hasan, S.Z. Hassan, T. Hassan Azmi, M.A. Rahman, M. Zavid Parvez, Deep learning based binary classification for Alzheimer's disease detection using brain MRI images, in: 2020 15th IEEE Conference on Industrial Electronics and Applications, ICIEA, IEEE, 2020, pp. 1115–1120.
[34] B. Tuvshinjargal, H. Hwang, VGG-C transform model with batch normalization to predict Alzheimer's disease through MRI dataset, Electronics 11 (2022) http://dx.doi.org/10.3390/electronics11162601.